ARTICLE

A Compact Apparatus for Gas-Phase Low-Temperature Kinetics Study Based on *de* Laval Nozzle

Feiyue Zhou[a,b], Jiale Zhang[a], Changmao Li[a], Wenrui Dong[a,b], Xueming Yang[a,b,c], Hongwei Li[a,b]*

a. State Key Laboratory of Chemical Reaction Dynamics and Dalian Coherent Light Source, Dalian Institute of Chemical Physics, Chinese Academy of Sciences, Dalian 116023, China
b. University of Chinese Academy of Sciences, Beijing 100049, China
c. Department of Chemistry and Center for Advanced Light Source Research, Southern University of Science and Technology, Shenzhen 518055, China

(Dated: Received on July 15, 2025; Accepted on September 8, 2025)

We have developed a compact apparatus to investigate low-temperature gas-phase reaction kinetics. This apparatus integrates pulsed *de* Laval nozzles with vacuum ultraviolet photoionization reflectron time-of-flight mass spectrometry (VUV-ReTOFMS) for sensitive detection of neutral–neutral reaction products. A uniform supersonic flow (M=3.56) was established in an N_2 nozzle, with measured temperature of (85.1±4.7) K and density of (4.49±0.60)×10^{16} molecule·cm^{-3}. The reaction between methylidyne radical (CH·) and propene (C_3H_6) was investigated using 118 nm VUV-ReTOFMS. A dominant C_4H_6+H product channel was observed, consistent with previous studies, demonstrating the product detection capability of the apparatus. This compact and sensitive instrument will be coupled with the Dalian Coherent Light Source (DCLS) to enable isomer-resolved product detection in low-temperature reactions.

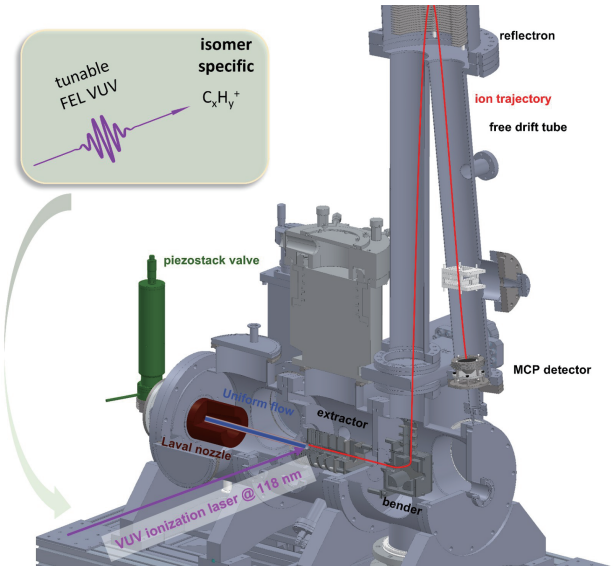

Key words: Gas-phase low-temperature reaction, Uniform supersonic flow, Radical–neutral reaction

I. INTRODUCTION

Simulating cold interstellar environments in the laboratory provides a direct approach to studying the chemical reaction kinetics and pathways that form complex reaction networks in cold dark clouds, star forming regions, pre-stellar cores, and protoplanetary disks [1–6]. It is well-established that interstellar chemistry occurs across a wide range of temperatures, from the cold (~10 K) environments of dark clouds such as TMC-1 [7], B1-b [8], and Barnard 68 [9], to the warmer conditions of regions like Sgr B2 (~50–70 K) [10], OMC-1 (~62 K) [11], quasar Q 0013-004 (~100 K) [12], and Orion Bar (~150 K) [13]. Radical–neutral reactions, which exhibit unconventional behavior in the interstellar medium (ISM), significantly contribute to chemical complexity and necessitate dedicated low-temperature

* Author to whom correspondence should be addressed.
E-mail: lihw@dicp.ac.cn

investigation [3, 4]. Recent advances in supersonic flow techniques, particularly the CRESU (Cinétique de Réaction en Écoulement Supersonique Uniforme) method employing *de* Laval nozzles, enable the generation of uniform gas flows at astrophysically relevant low temperatures [14–35]. In this approach, gases undergo isentropic expansion through a convergent–divergent nozzle, where the conversion of internal energy to translational energy produces a low-temperature uniform supersonic flow. While numerous kinetic studies of reactions between radicals (*e.g.*, C [15, 23], CN [19, 26], OH [17, 27], CH [21, 29]) and molecules have employed this technique, most focus exclusively on reaction rate coefficient measurements. These coefficients are crucial for quantifying reaction efficiencies in cold ISM environments. However, the experimental determination of reaction products— essential for refining astrochemical models of molecular evolution [36–38]—remains scarce.

The identification of reaction products also plays a central role in chemical reaction kinetics. The high number density (10^{16}–10^{17} molecule·cm^{-3}) characteristic of uniform supersonic flows from Laval nozzles facilitates species detection at low temperatures. The uniform flows have been successfully coupled with various spectroscopic [19, 20, 26] and mass spectrometric [16, 24, 25] techniques for product analysis. While rotational spectroscopic method offers near-universal molecular detection, challenges remain in detecting molecules with low permanent dipole moment and in developing efficient sampling methods for uniform flow studies. In contrast, mass spectrometry provides universal species detection. Successful integration of mass spectrometry with uniform flows has been demonstrated by Leone *et al.* [24] and Picard *et al.* [25], with tunable synchrotron light as a photoionization source for studies of Titan-relevant chemistry.

Building upon our previous instrument design [21, 30], we have developed a new, more compact, and highly sensitive VUV-ReTOFMS apparatus. This upgraded system integrates pulsed Laval nozzles with vacuum ultraviolet photoionization reflectron time-of-flight mass spectrometry (VUV-ReTOFMS), enabling the sensitive detection of reaction products and intermediates from neutral–neutral reactions under interstellar-relevant cold conditions. The enhanced sensitivity and movability of this design make it suitable for future coupling with the tunable Dalian Coherent Light Source (DCLS), which is essential for isomer detection and the study of species with high ionization energies. Section II details the instrument design, while Section III characterizes the uniform supersonic flow and presents photoionization mass spectra at 118.27 nm for the reaction between methylidyne (CH·) and propene (C_3H_6).

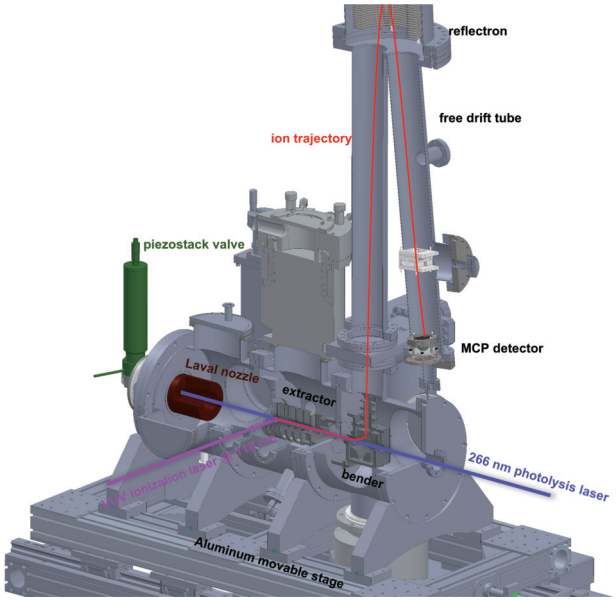

FIG. 1 Apparatus overview. Three-dimensional schematic of the compact low temperature kinetic apparatus based on piezostack pulse valve (green) and a Laval nozzle (cardinal). The photolysis laser (blue), VUV ionization laser (pink) and ion trajectory (red) are also shown. The aluminum mechanical stage and each part of ReTOFMS are also denoted (black).

II. APPARATUS OVERVIEW

We have developed a new experimental apparatus combining a pulsed Laval nozzle with vacuum ultraviolet (VUV) photoionization reflectron time-of-flight mass spectrometry (ReTOFMS). As shown in FIG. 1, the apparatus features a main cylindrical chamber (0.8 m in length and 0.3 m in diameter) housing the Laval nozzle, ion extractor, and quadrupole bender, along with a reflectron tube for enhanced mass resolution. An aluminum frame with mechanical translation stages enables precise vertical and horizontal alignment to optimize the overlap between the sampled uniform flow and the ionization laser beam. The entire apparatus incorporates vibration isolation from pumping systems.

A. Uniform flow chamber

A supersonic flow was generated through isentropic expansion of N_2 bath gas via a convergent–divergent

DOI: 10.1063/1674-0068/cjcp2507093

Laval nozzle (designed for 85 K) into the vacuum chamber. The internal nozzle profile was well designed to produce highly uniform Mach number (M), density (ρ) and temperature (T) distribution along the axis of the flow. The nozzle assembly was mounted onto a stainless-steel gas reservoir connected to a high-throughput piezostack pulsed valve (Coremorrow, PSt 150) operated at 10 Hz. Gas mixtures were introduced into the reservoir using high-accuracy mass flow controllers (MKS, GM50 series), maintaining at 32.5 Torr throughout the experiments. The main flow chamber was evacuated by a combination of dry pumps (Edwards, nXR60i and nXR200i) and a booster mechanical pump (Edwards, EH1200, pumping capacity$\approx$1200 m^3/h), achieving the required background pressure (~0.35 Torr) for stable supersonic expansion. Flow characterization employed two pressure transducers (Endveco, 8530C): a fixed transducer measuring stagnation pressure (P_0) upstream of the nozzle, and a second transducer mounted on a rotatable arm recording impact pressure (P_i) within the flow. A 266 nm photolysis laser (Beamtech, Nimma 900; Nd:YAG, fourth harmonic generation output) counter-propagated along the central flow axis, photolyzing $CHBr_3$ precursor (Sigma-Aldrich, 99%) to generate CH radical and initiate reaction.

B. VUV-ReTOFMS chamber

A skimmer (Beam dynamics, Model 2, 1 mm orifice) was positioned between the uniform flow chamber and the photoionization chamber of ReTOFMS to sample the isentropic core of the flow and establish differential pumping. Another 4 mm orifice was placed to separate the photoionization chamber and the ion-bending chamber. The latter houses a quadrupole bender, which is followed by a free drift tube, reflectron and a microchannel plate (MCP) detector. Both the photoionization and ion-bending chambers were evacuated by molecular pumps (Edwards, STP-A803C), each backed by a dry scroll pump (Edwards, nXR35i).

VUV radiation at 118.27 nm was generated by frequency tripling the 355 nm output from a Nd:YAG laser (Beamtech, Nimma-900) in a xenon gas cell. This photon energy enables ionization of most organic compounds without causing extensive fragmentation, thereby providing soft ionization for molecular identification. A 7-mm-off-axis LiF lens assembly downstream of the cell deflected and blocked residual 355 nm radiation that could otherwise interfere with ion detection. The VUV beam was spatially and temporally overlapped with the uniform flow in the ionization region, approximately 3 cm downstream from the skimmer tip to reduce diffusional losses. The extraction region, with a two-stage acceleration field design, consists of six annular electrode plates (1 mm thickness, 86 mm outer diameter and 20 mm inner diameter). The first acceleration stage consists of two plates separated by 10 mm, with the ionization center positioned midway between them, while the second stage incorporates five equally spaced plates with 5 mm intervals.

A quadrupole bender was designed to redirect ions by 90° upward into an 890-mm-long free drift region. A set of Einzel lens and deflection plates were coupled to the bender to focus and align ions. The reflectron, containing 41 annular electrodes with a two-stage deceleration electric field, doubles the flight distance and compensates for initial ion velocity dispersion, thereby enhancing mass resolution. A Z-stack microchannel plate (MCP) detector collected all ions, with signals amplified by a preamplifier (Femto, DHPCA-100) and digitized by an analog-to-digital converter (Fcctec Technology, USB9982C). A custom LabVIEW program controlled data acquisition and analysis, and all timing sequences—including the pulsed valve, laser systems, and ADC—were synchronized by a delay generator (Quantum Composers, 9528).

III. RESULTS

A. Flow condition characterization

The Laval nozzle was designed to convert high-pressure reservoir gas into a well-defined, uniform supersonic flow through isentropic expansion. This method creates a wall-less environment ideal for studying low-temperature reaction kinetics. Flow uniformity along the axis was characterized using Pitot measurements. Two pressure transducers were employed: one positioned to measure impact pressure (P_i) along the flow axis, and the other to record static pressure (P_0) upstream of the nozzle entrance. The relationship between P_i and P_0 follows the Rayleigh Pitot formula [39]:

$$\frac{P_i}{P_0} = \left[\frac{(\gamma+1)M^2}{(\gamma-1)M^2+2}\right]^{\frac{\gamma}{\gamma-1}} \left(\frac{\gamma+1}{2\gamma M^2-\gamma+1}\right)^{\frac{1}{\gamma-1}} \quad (1)$$

where M is the Mach number of the flow and γ is the heat capacity ratio ($\gamma = C_p/C_v$, γ=1.667 for He and Ar,

DOI: 10.1063/1674-0068/cjcp2507093

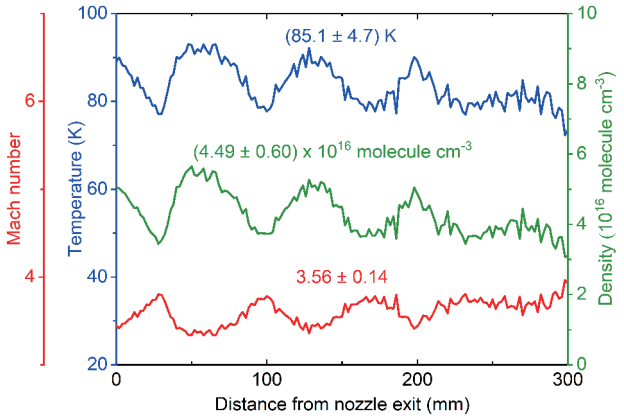

FIG. 2 The flow conditions of 85 K N_2 nozzle characterized by Pitot measurements along the nozzle axis. The flow profile of Mach number (red), temperature (blue), and density (green) are depicted. Temperature, density, and Mach number were obtained from statistical analysis of experimental measurements taken over the first 200 mm length. The uncertainty corresponds to 1σ from the mean of all values obtained along the uniform flow axis.

1.4 for N_2). This equation shows extreme sensitivity to Mach number variations, making the Pitot measurement (P_i) an excellent metric for assessing flow uniformity. An iterative procedure was employed, where trial values of M were substituted into Eq.(1) until the solution converged within the specific tolerance. Then temperature (T), pressure (P), and density (ρ) of the post-nozzle supersonic flow were determined from the derived Mach number using Eqs. (2), (3), and (4),

$$\frac{T}{T_0} = \left[1 + \left(\frac{\gamma - 1}{2}\right) M^2\right]^{-1} \tag{2}$$

$$\frac{P}{P_0} = \left[1 + \left(\frac{\gamma - 1}{2}\right) M^2\right]^{\frac{-\gamma}{\gamma - 1}} \tag{3}$$

$$\frac{\rho}{\rho_0} = \left[1 + \left(\frac{\gamma - 1}{2}\right) M^2\right]^{\frac{-1}{\gamma - 1}} \tag{4}$$

where T_0 and ρ_0 are temperature and density in the static pressure region, respectively. To characterize the flow, the Pitot tube was translated axially downstream from the nozzle exit to record P_i, from which a flow condition profile was determined as shown in FIG. 2. In the present configuration, the uniform zone extends ~20 cm downstream from the nozzle exit, corresponding to a chemical reaction time window of ~300 μs. The temperature and density in this region were measured to be (85.1±4.7) K and $(4.49\pm0.60)\times10^{16}$ molecule·cm^{-3}, respectively.

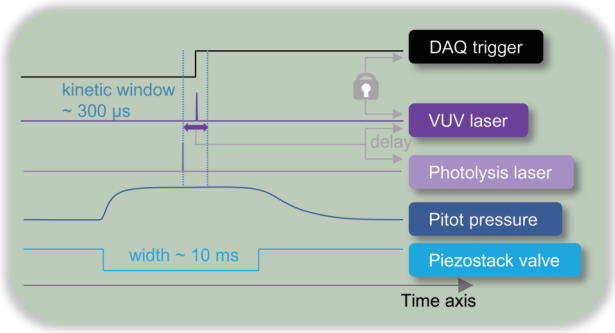

FIG. 3 Timing of all components that are in precise control synchronized via a delay generator. As photolysis laser is fixed at the middle of the plateau of Pitot pressure profile, the cascaded delays of VUV probe laser form a maximum kinetic window of about 300 μs. The DAQ trigger is synchronized to the VUV probe laser.

B. Timing control

The apparatus was operated in a pulsed mode and precisely synchronized using an eight-channel digital delay generator. As shown in FIG. 3, a TTL signal (typically 10 ms wide) first triggered the pulsed valve, initiating gas expansion to establish the uniform supersonic flow. This produced a 7-ms pressure plateau within the flow. The photolysis laser, which produces radicals and initiates the reaction, was fired at the middle of the plateau (defined as $t=0$). The VUV probe laser was delayed by Δt, corresponding to the reaction time. For photolysis-probe experiments, multiple laser delays were cascaded through the delay generator to map a kinetic window spanning up to 300 μs. The ADC card was synchronized with the VUV pulse for data acquisition.

C. Mass spectrometry validation

The homemade reflectron time-of-flight mass spectrometer (ReTOFMS), integrated with the pulsed supersonic uniform flow in our apparatus, demonstrated robust performance in resolving reaction products with high sensitivity and good mass resolution. The 3 cm distance between the skimmer sampling point and photoionization interaction region is shorter than in the previous 5 cm design [21], enhancing product ion signals due to increased molecular density at shorter distances. Two-stage extraction fields (440 V·cm^{-1} and 660 V·cm^{-1}) ensured efficient ion collection while compensating for the spatial divergence due to the beam size of the VUV photoionization laser [40]. The nascent

DOI: 10.1063/1674-0068/cjcp2507093

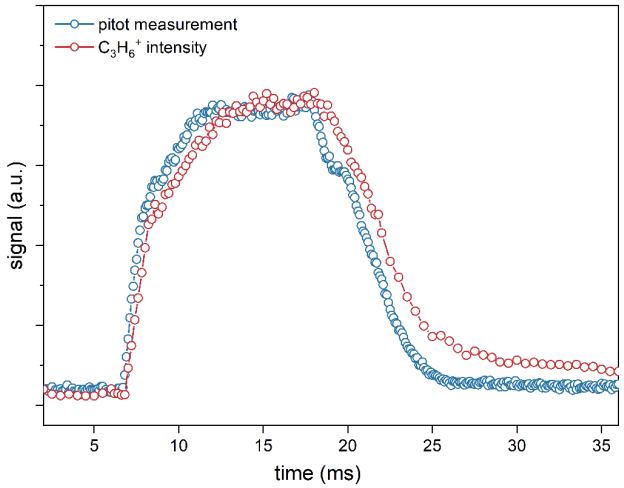

FIG. 4 Raw flow pressure curve (blue) by the Pitot measurement and the sampled $C_3H_6^+$ profile (red) by the ReTOFMS measurement.

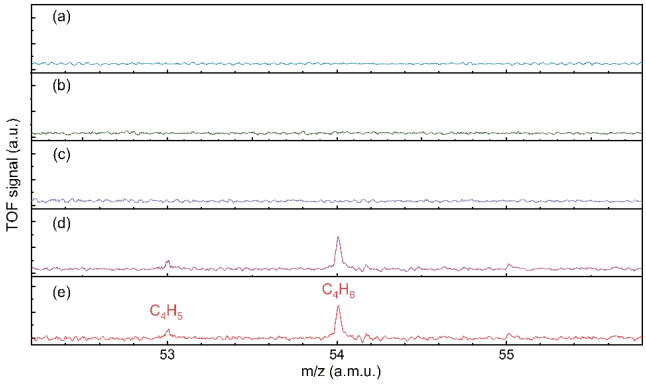

FIG. 5 Mass spectra for CH·+C_3H_6 reaction product detection under different conditions at a kinetic time of 100 μs. (a) $CHBr_3$ only, with 266 nm photolysis laser on; (b) C_3H_6 only, with 266 nm photolysis laser on; (c) both $CHBr_3$ and C_3H_6 present, with 266 nm photolysis laser off; (d) both $CHBr_3$ and C_3H_6 present, with 266 nm photolysis laser on; and (e) subtraction of spectrum (c) from spectrum (d).

reaction products sampled by the skimmer exhibit velocity spread along the ion acceleration axis, which would degrade mass resolution [41]. To address this, the reflectron was incorporated with a two-stage electrostatic configuration (129 V·cm^{-1} and 69 V·cm^{-1}), achieving a mass resolution ($m/\Delta m$) > 600 (FWHM) at m/z 42. This resolution enables unambiguous identification of reaction products and intermediates.

FIG. 4 shows a comparison between the pulsed gas profile obtained from Pitot measurement and the skimmer-sampled mass signal of $C_3H_6^+$ from ReTOFMS measurement. Both signals exhibit similar temporal profiles, gradually rising to a plateau and then dropping as the pulsed valve closed. The rise and fall times are determined by the electrical response of the pulsed piezostack valve, while the plateau duration can be adjusted by controlling the valve opening time. The excellent agreement between these profiles demonstrates that our custom ReTOFMS effectively samples the uniform flow while preserving kinetic information about reaction intermediates and products with minimal perturbation from thermalized gases reflected by the skimmer, which is crucial for reaction kinetics studies.

The reaction between ground-state CH radicals and propene (C_3H_6) was investigated in a uniform supersonic flow at 85.1 K. The flow contained bromoform ($CHBr_3$) with a density of 5×10^{13} molecule·cm^{-3}, and propene at 1.5×10^{14} molecule·cm^{-3}. Given the absorption cross-section of $CHBr_3$ at 266 nm is similar to that at 248 nm [42, 43], and with a photolysis laser flux of 65 mJ·cm^{-2}, the CH radical concentration was estimated to be 2×10^{10} molecule·cm^{-3} using the yield of $(5\pm2.5)\times10^{-4}$ as reported by Romanzin *et al.* [44]. Reaction products were ionized by a 118 nm VUV pulse (delayed by 100 μs after photolysis) and detected by ReTOFMS.

Product identification required careful discrimination from background signals (carrier gas, radical precursors, propene, and photolysis/ionization fragments), accomplished through systematic comparison of spectra obtained under four conditions: (i) $CHBr_3$ only, (ii) propene only, (iii) both reactants without photolysis, and (iv) both reactants with photolysis. FIG. 5 displays distinct product mass spectra featuring two ion peaks at m/z 53 and 54, consistent with previous findings [21]. Similar product ion signal levels were obtained under the same experimental conditions but with a much lower gain on the MCP detector (only a 2100 V voltage difference was applied rather than 2500 V before). These products form via barrierless CH radical attack on propene, generating highly energized C_4H_7 intermediates that undergo rapid isomerization prior to H/H_2 elimination. The dominant C_4H_6 product channel (m/z 54) agrees with theoretical predictions [45–48] showing 1,3-butadiene as the primary isomer under room temperature. Synchrotron-based photoionization mass spectrometry (PIMS) studies at 298 K and 4 Torr experimentally confirmed 1,3-butadiene, 1,2-butadiene, and 1-butyne as major products [49]. In contrast, crossed molecular beam (CMB) studies under single-collision conditions suggested the cyclic isomers 1-

DOI: 10.1063/1674-0068/cjcp2507093

methylcyclopropene and 3-methylcyclopropene as the dominant nascent products [50]. Although the current experimental setup cannot distinguish between these C_4H_6 isomers due to the fixed VUV wavelength, future integration with a tunable VUV source (*e.g.*, DCLS) will facilitate isomer-resolved product analysis in low-temperature kinetics studies.

IV. CONCLUSION

We present a new compact and sensitive apparatus for investigating gas-phase reaction kinetics at low temperatures (~85 K) relevant to interstellar environments. This apparatus integrates pulsed Laval nozzles with vacuum ultraviolet photoionization reflectron time-of-flight mass spectrometry (VUV-ReTOFMS) for sensitive detection of neutral–neutral reaction products. Using 118 nm photoionization, we investigated the reaction between methylidyne radicals (CH·) and propene (C_3H_6), observing a dominant C_4H_6 +H product channel, consistent with previous studies. Notably, comparable product ion signals were achieved with significantly reduced MCP detector gain. This compact, high-sensitivity instrument will be coupled with the Dalian Coherent Light Source (DCLS) to enable isomer-resolved product detection in low-temperature reactions.

V. ACKNOWLEDGMENTS

The authors gratefully acknowledge the Dalian Coherent Light Source (DCLS) for support and assistance. This work was supported by the National Natural Science Foundation of China (No.22273103), the National Natural Science Foundation of China (NSFC Center for Chemical Dynamics) (No.22288201), Dalian Institute of Chemical Physics (DICP I202230).

[1] I. W. M. Smith and B. R. Rowe, Acc. Chem. Res. **33**, 261 (2000).
[2] B. Hansmann and B. Abel, ChemPhysChem **8**, 343 (2007).
[3] M. A. Blitz and P. W. Seakins, Chem. Soc. Rev. **41**, 6318 (2012).
[4] A. Potapov, A. Canosa, E. Jiménez, and B. Rowe, Angew. Chem. Int. Ed. **56**, 8618 (2017).
[5] L. Wiesenfeld, J. Oomens, and A. S. C. Cheung, Phys. Chem. Chem. Phys. **20**, 5341 (2018).
[6] I. R. Cooke and I. R. Sims, ACS Earth Space Chem. **3**, 1109 (2019).
[7] P. Pratap, J. E. Dickens, R. L. Snell, M. P. Miralles, E. A. Bergin, W. M. Irvine, and F. P. Schloerb, Astrophys. J. **486**, 862 (1997).
[8] K. I. R. Öberg, S. Bottinelli, J. K. Jorgensen, and E. F. van Dishoeck, Astrophys. J. **716**, 825 (2010).
[9] S. Hotzel, J. Harju, and M. Juvela, Astron. Astrophys. **395**, L5 (2002).
[10] A. Sánchez-Monge, P. Schilke, A. Schmiedeke, A. Ginsburg, R. Cesaroni, D. C. Lis, S. L. Qin, H. S. P. Müller, E. Bergin, C. Comito, and T. Möller, Astron. Astrophys. **604**, A10 (2017).
[11] X. D. Tang, C. Henkel, K. M. Menten, F. Wyrowski, N. Brinkmann, X. W. Zheng, Y. Gong, Y. X. Lin, J. Esimbek, J. J. Zhou, Y. Yuan, D. L. Li, and Y. X. He, Astron. Astrophys. **609**, A12 (2018).
[12] P. Petitjean, R. Srianand, and C. Ledoux, Mon. Not. R. Astron. Soc. **332**, 383 (2002).
[13] W. Batrla and T. L. Wilson, Astron. Astrophys. **408**, 231 (2003).
[14] B. R. Rowe, G. Dupeyrat, J. B. Marquette, and P. Gaucherel, J. Chem. Phys. **80**, 4915 (1984).
[15] D. Chastaing, P. L. James, I. R. Sims, and I. W. M. Smith, Phys. Chem. Chem. Phys. **1**, 2247 (1999).
[16] S. Lee, R. J. Hoobler, and S. R. Leone, Rev. Sci. Instrum. **71**, 1816 (2000).
[17] S. E. Taylor, A. Goddard, M. A. Blitz, P. A. Cleary, and D. E. Heard, Phys. Chem. Chem. Phys. **10**, 422 (2008).
[18] J. Daranlot, M. Jorfi, C. J. Xie, A. Bergeat, M. Costes, P. Caubet, D. Q. Xie, H. Guo, P. Honvault, and K. M. Hickson, Science **334**, 1538 (2011).
[19] C. Abeysekera, L. N. Zack, G. B. Park, B. Joalland, J. M. Oldham, K. Prozument, N. M. Ariyasingha, I. R. Sims, R. W. Field, and A. G. Suits, J. Chem. Phys. **141**, 104307 (2014).
[20] D. I. Lucas, T. Guillaume, D. E. Heard, and J. H. Lehman, J. Chem. Phys. **161**, 044302 (2024).
[21] F. Y. Zhou, S. Z. Ma, L. Li, J. L. Zhang, C. L. Xiao, W. R. Dong, and H. W. Li, J. Chem. Phys. **162**, 094201 (2025).
[22] N. A. West, T. J. Millar, M. Van de Sande, E. Rutter, M. A. Blitz, L. Decin, and D. E. Heard, Astrophys. J. **885**, 131 (2019).
[23] K. M. Hickson, J. C. Loison, and V. Wakelam, ACS Earth Space Chem. **9**, 1679 (2025).
[24] S. Soorkia, C. L. Liu, J. D. Savee, S. J. Ferrell, S. R. Leone, and K. R. Wilson, Rev. Sci. Instrum. **82**, 123106 (2011).
[25] O. Durif, M. Capron, J. P. Messinger, A. Benidar, L. Biennier, J. Bourgalais, A. Canosa, J. Courbe, G. A. Garcia, J. F. Gil, L. Nahon, M. Okumura, L. Rutkowski, I. R. Sims, J. Thiévin, and S. D. Le Picard, Rev. Sci. Instrum. **92**, 053110 (2021).
[26] N. Suas-David, S. Thawoos, and A. G. Suits, J. Chem.

Phys. **151**, 124303 (2019).
[27] R. J. Shannon, M. A. Blitz, A. Goddard, and D. E. Heard, Nat. Chem. **5**, 745 (2013).
[28] B. M. Hays, D. Gupta, T. Guillaume, O. Abdelkader Khedaoui, I. R. Cooke, F. Thibault, F. Lique, and I. R. Sims, Nat. Chem. **14**, 811 (2022).
[29] P. Bocherel, L. B. Herbert, B. R. Rowe, I. R. Sims, I. W. M. Smith, and D. Travers, J. Phys. Chem. **100**, 3063 (1996).
[30] S. Ma, F. Zhou, G. Sun, C. Xiao, W. Dong, H. Li, and X. Yang, Chin. J. Chem. Phys. **38**, 249 (2025).
[31] S. Thawoos, N. Suas-David, R. M. Gurusinghe, M. Edlin, A. Behzadfar, J. Lang, and A. G. Suits, J. Chem. Phys. **159**, 034304 (2023).
[32] B. Schläppi, J. H. Litman, J. J. Ferreiro, D. Stapfer, and R. Signorell, Phys. Chem. Chem. Phys. **17**, 25761 (2015).
[33] N. Daugey, P. Caubet, B. Retail, M. Costes, A. Bergeat, and G. Dorthe, Phys. Chem. Chem. Phys. **7**, 2681 (2005).
[34] M. Tizniti, S. D. Le Picard, F. Lique, C. Berteloite, A. Canosa, M. H. Alexander, and I. R. Sims, Nat. Chem. **6**, 141 (2014).
[35] E. Jiménez, B. Ballesteros, A. Canosa, T. M. Townsend, F. J. Maigler, V. Napal, B. R. Rowe, and J. Albaladejo, Rev. Sci. Instrum. **86**, 043102 (2015).
[36] J. C. Loison, V. Wakelam, K. M. Hickson, A. Bergeat, and R. Mereau, Mon. Not. R. Astron. Soc. **437**, 930 (2013).
[37] V. Wakelam, P. Gratier, J. C. Loison, K. M. Hickson, J. Penguen, and A. Mechineau, Astron. Astrophys. **689**, A101 (2024).
[38] T. J. Millar, C. Walsh, M. Van de Sande, and A. J. Markwick, Astron. Astrophys. **682**, A42 (2024).
[39] G. Dupeyrat, J. B. Marquette, and B. R. Rowe, Phys. Fluids **28**, 1273 (1985).
[40] W. C. Wiley and I. H. McLaren, Rev. Sci. Instrum. **26**, 1150 (1955).
[41] M. Guilhaus, D. Selby, and V. Mlynski, Mass Spectrom. Rev. **19**, 65 (2000).
[42] D. K. Papanastasiou, S. A. McKeen, and J. B. Burkholder, Atmos. Chem. Phys. **14**, 3017 (2014).
[43] D. Gillotay, A. Jenouvrier, B. Coquart, M. F. Merienne, and P. C. Simon, Planet Space Sci. **37**, 1127 (1989).
[44] C. Romanzin, S. Boyé-Peronne, D. Gauyacq, Y. Bénilan, M. C. Gazeau, and S. Douin, J. Chem. Phys. **125**, 084308 (2006).
[45] J. L. Miller, J. Phys. Chem. A **108**, 2268 (2004).
[46] Y. Li, H. L. Liu, Z. J. Zhou, X. R. Huang, and C. C. Sun, J. Phys. Chem. A **114**, 9496 (2010).
[47] J. M. Ribeiro and A. M. Mebel, J. Phys. Chem. A **120**, 1800 (2016).
[48] J. C. Loison and A. Bergeat, Phys. Chem. Chem. Phys. **11**, 655 (2009).
[49] A. J. Trevitt, M. B. Prendergast, F. Goulay, J. D. Savee, D. L. Osborn, C. A. Taatjes, and S. R. Leone, J. Phys. Chem. A **117**, 6450 (2013).
[50] C. He, A. M. Thomas, G. R. Galimova, A. M. Mebel, and R. I. Kaiser, J. Phys. Chem. A **123**, 10543 (2019).

DOI: 10.1063/1674-0068/cjcp2507093